High-temperature Raman spectroscopic and X-ray diffraction study of β-Mg$_2$SiO$_4$: Insights into its high-temperature thermodynamic properties and the β- to α-phase-transformation mechanism and kinetics

BRUNO REYNARD,[1] FOUZIA TAKIR,[1] FRANÇOIS GUYOT,[2],* GABRIEL D. GWANMESIA,[2]
ROBERT C. LIEBERMANN,[2] AND PHILIPPE GILLET[3]

[1]Géosciences Rennes CNRS UPR 4661, Institut de Géologie, Université de Rennes 1, 35042 Rennes Cedex, France
[2]Center for High Pressure Research and Mineral Physics Institute, State University of New York at Stony Brook,
Stony Brook, New York 11794-2100, U.S.A.
[3]Laboratoire des Sciences de la Terre, Ecole Normale Supérieure, CNRS URA 726, 46 Allée d'Italie, 69364 Lyon Cedex 07, France

ABSTRACT

We performed in-situ Raman spectroscopy and X-ray diffraction experiments at high temperature and ambient pressure to investigate the intrinsic anharmonic properties of β-Mg$_2$SiO$_4$ and the mechanism and kinetics of its back-transformation to forsterite. High-temperature Raman spectra of β-Mg$_2$SiO$_4$ and its back-transformed products were recorded up to 1200 K. β-Mg$_2$SiO$_4$ persists metastably up to 800–900 K, and the Raman frequency shifts with temperature were determined. Between 800 and 1000 K, new peaks are observed at about 670 and 1020 cm^{-1}. Above 1000 K, a direct transformation to forsterite occurs. The peaks that appear between 800 and 1000 K are attributed to a defective spinelloid that forms as an intermediate phase during the back-transformation of β-Mg$_2$SiO$_4$ to forsterite. Similar features are observed in the Raman spectrum of partially transformed γ-Ni$_2$SiO$_4$ heated at 1073 K and ambient pressure for 10 min. These results indicate that a two-step mechanism, possibly martensitic, is operative in the back-transformation of the β- and γ-phases to olivine at low to moderate temperatures and for a large overstepping of the equilibrium conditions.

The kinetics of the β- to α-Mg$_2$SiO$_4$ back-transformation were monitored between 1023 and 1120 K at ambient pressure using X-ray powder diffraction. For the kinetic data obtained in air, two regimes are evident from an Avrami analysis. The first regime is characterized by an exponent $n \approx 2$ for a low transformed fraction ($X < 0.5$); the second has $n \approx 1$ for higher transformed fractions. For this second regime, an activation energy of 432 ± 64 kJ/mol is derived for the growth process from the kinetic data. A smaller data set collected in vacuum indicates much slower transformation rates and suggests a significant effect of the O$_2$ or H$_2$O partial pressures on the kinetics.

Intrinsic mode anharmonic parameters can be calculated from the Raman frequency shifts with temperature and used to correct vibrational heat capacity models for intrinsic anharmonic effects. These corrections are slightly higher for the β-phase than for forsterite but the difference is within the experimental error. This indicates that, within the resolution of our experiments, no significant effect of intrinsic anharmonicity on the location and slope of the α-β phase transition can be predicted.

INTRODUCTION

β-Mg$_2$SiO$_4$, a high-pressure polymorph of forsterite (α-Mg$_2$SiO$_4$), is believed to be a major phase of the Earth's mantle at depths between 410 and 520 km. The density and seismic-wave velocity jumps at the 410 km discontinuity are attributed to the α-β transformation in olivine-rich models of the mantle (e.g., Akaogi et al. 1989; Katsura and Ito 1989). Yet few studies have characterized

the high-temperature properties of the β-phase. Suzuki et al. (1980) measured its thermal expansivity at 1 bar up to 1073 K by X-ray diffraction. In a high-temperature, single-crystal X-ray diffraction study, Tsukimura et al. (1988) determined the thermal expansion as well as the back-transformation reaction up to 1100 K. Watanabe (1982) measured the specific heat up to 700 K. In this study, we present an in-situ high-temperature Raman spectroscopic study of β-Mg$_2$SiO$_4$. The purpose of the study is twofold: to measure the intrinsic anharmonicity of the β-phase and present new data on the mechanism of the back-transformation to forsterite. The determination of intrinsic anharmonicity is important because it

influences the high temperature (>1000 K) thermody-
namic properties, such as the specific heat and the entro-
py (Gillet et al. 1989, 1991). In particular, it is essential
for phase diagram calculations at high temperatures to
determine whether intrinsic anharmonicity is different in
the β-phase and forsterite.

The mechanism and kinetics of the β- to α-Mg$_2$SiO$_4$
transformation are important for understanding the pres-
ervation of wadsleyite in meteorites, and the microstruc-
tures contained therein (e.g., Price et al. 1983; Price 1983;
Madon and Poirier 1983), as well as the possible occur-
rence of wadsleyite as ultradeep inclusions in diamonds.
The study of the β- to α-Mg$_2$SiO$_4$ transformation at 1 bar
also provides the opportunity to investigate a reaction
closely related to the olivine-spinel transformation *sensu
lato* in a condition far from equilibrium and in the ab-
sence of deviatoric stresses usually present in high-pres-
sure experiments. Indeed, in addition to heterogeneous
nucleation and growth mechanisms, it has been proposed
that the olivine-spinel *sensu lato* transition occurs by
shear-assisted ("martensitic") mechanisms involving spi-
nelloids (Poirier 1981a, 1981b; Hyde et al. 1982; Madon
and Poirier 1983). To investigate the nature of the tran-
sition mechanism and kinetics, experimental studies of
the olivine-spinel *sensu lato* phase transition have been
performed in analog systems, such as Mg$_2$GeO$_4$ (e.g.,
Vaughan et al. 1982, 1984; Rubie and Champness 1987;
Will and Lauterjung 1987; Burnley and Green 1989),
Ni$_2$SiO$_4$ (e.g., Boland and Liebermann 1983; Rubie et al.
1990), Fe$_2$SiO$_4$ (Lacam et al. 1980), and Co$_2$SiO$_4$ (Rems-
berg et al. 1988), and in the (Mg,Fe)$_2$SiO$_4$ system (Boland
and Liu 1983; Madon et al. 1989; Guyot et al. 1991;
Brearley et al. 1992). In general, experiments performed
in diamond-anvil cells with large deviatoric stresses (La-
cam et al. 1980; Boland and Liu 1983; Madon et al. 1989)
provided evidence for a martensitic mechanism, whereas
experiments conducted in large-volume apparatus
(Vaughan et al. 1982, 1984; Boland and Liebermann 1983;
Rubie and Champness 1987; Remsberg et al. 1988;
Brearley et al. 1992) under lower deviatoric-stress con-
ditions gave no evidence for a martensitic mechanism but
rather showed evidence for an incoherent nucleation and
growth mechanism. Burnley and Green (1989) showed
that the martensitic mechanism is actually favored by
high nonhydrostatic stresses with respect to an incoherent
nucleation mechanism activated under low differential
stress conditions. The study of the β- to α-Mg$_2$SiO$_4$ trans-
formation may help to decipher the respective effects of
nonequilibrium and nonhydrostaticity.

EXPERIMENTAL METHODS

Sample synthesis

Pure synthetic forsterite powder was used as a starting
material. This powder was compressed and heated in a
uniaxial split-sphere apparatus (USSA-2000), using the
cell assembly described in Gwanmesia et al. (1990). The
powder was first compressed slowly up to 15 GPa. Tem-
perature was then increased slowly up to 1273 K and held

for 1 h. The experiment was quenched by switching off
the input current, and then the pressure was slowly de-
creased. Quenched samples appear as cylinders of well-
sintered material about 1.5 mm in diameter and 2 mm
long. Samples were confirmed by X-ray diffraction to be
pure β-Mg$_2$SiO$_4$. The Ni$_2$SiO$_4$ spinel is the same sample
used by Reynard (1993) for infrared spectroscopic mea-
surements.

Raman spectroscopy

Raman spectra were recorded on a multichannel XY
DILOR microprobe at the University of Rennes. The Ra-
man signal was excited using either the 488 or 514.5 nm
lines of an Ar Spectra-Physics laser. Spectra were col-
lected in the 180° backscattering geometry through an
Olympus ULWD 50 objective (focal distance 8 mm, nu-
merical aperture 0.63). The laser light is focused onto a
spot <5 μm in diameter on the sample. The Raman light
is focused into a double-subtractive spectrometer and an-
alyzed by a CCD EGG-Ortec detector. Raman spectra at
high temperature were obtained in two ways: First, it was
observed that the presence of poorly crystalline graphite
in the sample (broad bands at 1360 and 1590 cm^{-1}) leads
to a temperature increase because of absorption of the
laser light. By varying the laser power it was possible to
obtain spectra at different temperatures (Expt. 1) with a
strong signal (the higher the laser power, the stronger the
signal and the higher the temperature). Rough estimates
of the temperature were obtained from the vibrational-
frequency shifts with temperature measured indepen-
dently for forsterite (Gillet et al. 1991) and β-Mg$_2$SiO$_4$
(see below). Temperatures of $\sim 1200 \pm 100$ K were ob-
tained using this method. Second, high-temperature spec-
tra were obtained using a Leitz 1350 heating stage. Tem-
peratures were measured with a Pt-Pt 10% Rh
thermocouple calibrated against melting points of stan-
dard compounds. To avoid sample heating from the la-
ser, a low laser power was used (50 mW at the laser out-
put leading to <5 mW at the sample). No frequency shifts
were observed at lower powers (the temperature increase
was estimated to be <50 K), but this procedure has a low
Raman signal-to-noise ratio. This laser power was kept
constant to allow comparison between spectra obtained
at different nominal temperatures indicated by the ther-
mocouple readings. The frequency shift with temperature
obtained for the most intense Raman mode of the β-phase
at 918 cm^{-1} was used to estimate temperatures for the
spectra obtained using the high laser power (Expt. 1).

X-ray diffraction and TEM

High-temperature powder-diffraction spectra were ob-
tained using a SCINTAG X-ray diffractometer equipped
with a standard goniometer. High temperatures were pro-
duced by the resistive heating of a platinum strip on which
the crushed sample was placed. The temperature was
monitored by a Pt-Pt 10% Rh thermocouple. Some ex-
periments were conducted under a vacuum of 10^{-2} Pa.
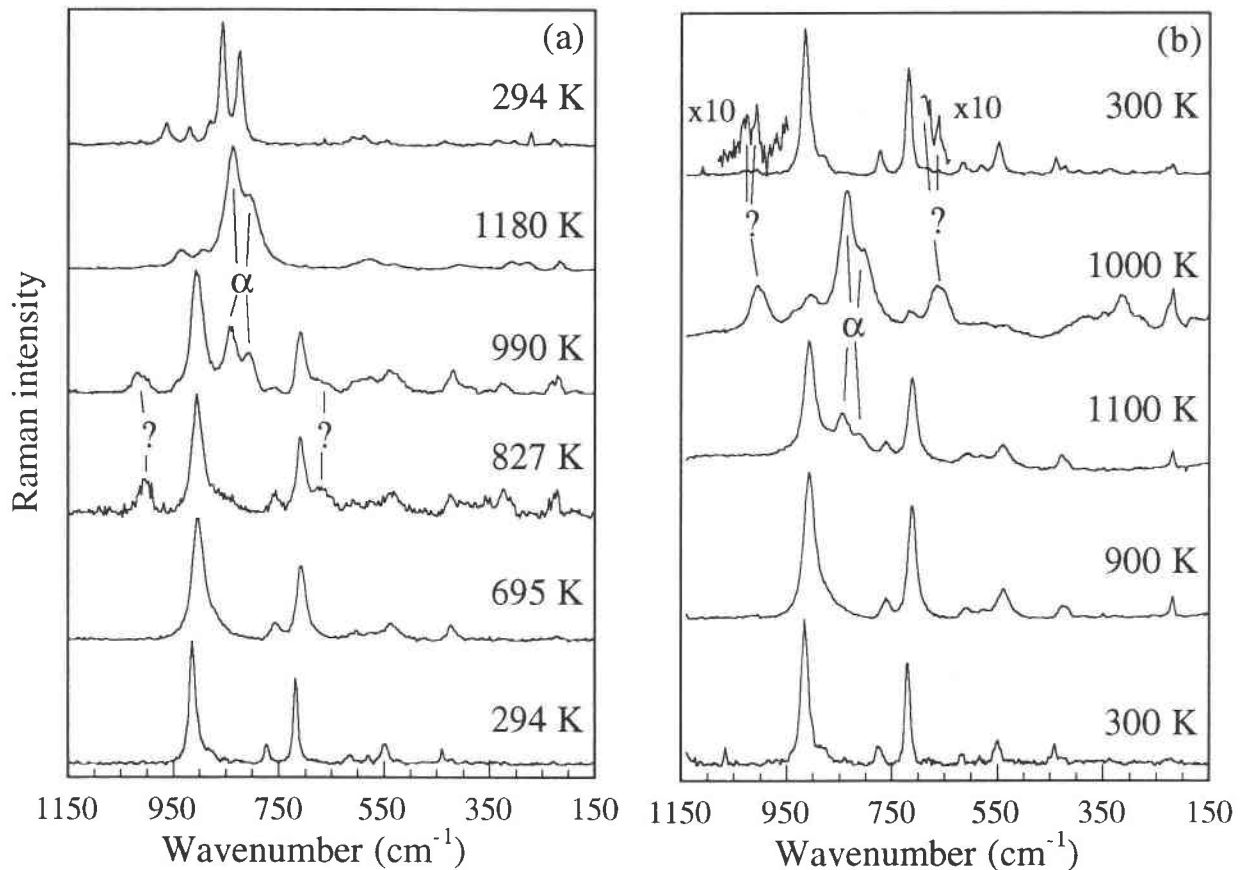The kinetics of the back-transformation of the β-phase to

FIGURE 1. High-temperature Raman spectra. **(a)** Experiments 2 and 3, from bottom to top: two spectra of untransformed β-Mg$_2$SiO$_4$ at 294 and 695 K; onset of the transformation at 827 K marked by the appearance of two broad peaks (labeled by question marks) that cannot be attributed to either β-Mg$_2$SiO$_4$ or forsterite; at temperatures close to 1000 K forsterite peaks (labeled α) appear and grow at the expense of all other peaks; at 1180 K, the transformation is nearly complete and forsterite is quenched. **(b)** Experiment 1, from bottom to top: two spectra of untransformed β-Mg$_2$SiO$_4$ at 300 and 900 K; onset of the direct transformation at about 1100 K, no extra peaks at 670 and 1020 cm^{-1} are observed; partially transformed β-Mg$_2$SiO$_4$ at about 1000 K, extra peaks at 670 and 1020 cm^{-1} are observed; β-Mg$_2$SiO$_4$ quenched from about 900 K, weak extra peaks are observed as doublets at 665–685 and 1005–1025 cm^{-1}.

olivine were determined quantitatively. The relative proportions of the β-phase and olivine were estimated from the X-ray spectra by summing the integrated intensities of the distinct peaks for each phase, with the assumption that the ratio of the abundances is similar to the ratio of the summed intensities. Using the summed intensities of several distinct peaks prevents any bias because of anisotropy or preferential orientation. Because this method requires good counting statistics, it was impossible to perform in-situ experiments at high temperature. Therefore we used the following procedure: (1) The sample was heated quickly (within 2 min) to the desired temperature; (2) it was maintained at this temperature for a short interval (typically 15 min); (3) the power in the furnace was then switched off, and the sample quenched within a few seconds to temperatures at which the transformation rate is nil at the scale of the experiment; (4) the X-ray spec-

trum was then collected from 15 to 40° 2θ for 2 h. This procedure was repeated until significant conversion to forsterite was observed.

TEM studies were performed on a JEOL 2000EX operating at 200 kV at the University of Rennes.

RESULTS

Raman spectroscopy

The Raman spectrum of β-Mg$_2$SiO$_4$ has been recorded at both ambient (McMillan and Akaogi 1987) and high pressures (Chopelas 1991). Our ambient temperature spectra of β-Mg$_2$SiO$_4$ (Fig. 1) from 146 to 945 cm^{-1} are consistent with these previous studies. Outside this frequency range, we did not observe the low-frequency peak at 86 cm^{-1} (Chopelas 1991) and the weak high frequency peaks at 1100 cm^{-1} (McMillan and Akaogi 1987) and
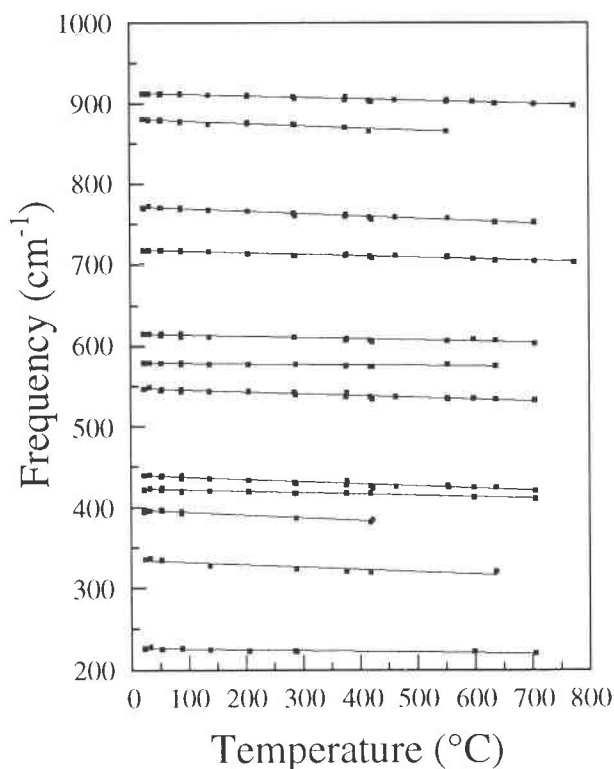
FIGURE 2. Temperature dependence of Raman frequencies of β-Mg$_2$SiO$_4$. The highest temperature points were obtained after back-transformation had started.
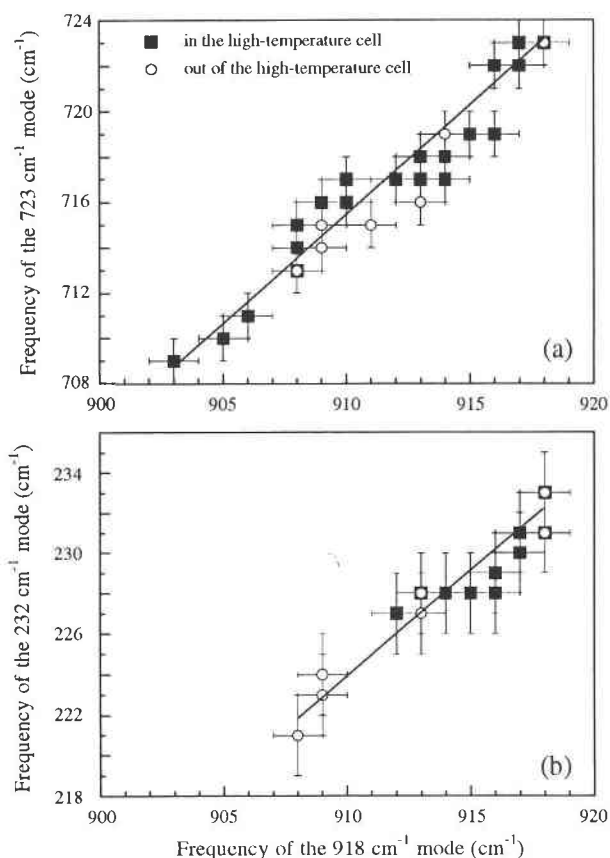

FIGURE 3. The mode frequencies obtained at different temperatures in (Expts. 2 and 3) and out (Expt. 1) of the high-temperature stage plotted relative to the most intense band of β-Mg$_2$SiO$_4$ (918 cm^{-1}). (**a**) Plot of the intense mode at 723 cm^{-1} shows good agreement between the two types of data. (**b**) The weak mode at 234 cm^{-1} shows an improved accuracy in the slope determination.

1020 cm^{-1} (Chopelas 1991), possibly because of the low signal-to-noise ratio in our spectra.

Two series of experiments were performed in the high-temperature cell (Fig. 1a). In the first series (Expt. 2), β-Mg$_2$SiO$_4$ was heated to 1180 K, in steps of 70–100 K and about 10 min at each step. In the second series (Expt. 3), the cell was heated to 830 K in steps of about 15–20 min each. Up to 900 K in Experiment 2 and 800 K in Experiment 3, either no transformation was observed, or it was sluggish in nature. Systematic frequency shifts with temperature were shown in Figure 2. For the less intense, low-frequency modes, the data obtained with high laser power outside of the high-temperature stage (Fig. 1b, Expt. 1) are more reliable because of their higher signal-to-noise ratio. They were combined with the data obtained in the high-temperature cell in the following way: (1) The frequency shift with temperature of the 918 cm^{-1} band, which has the greatest intensity, was chosen as a reference; (2) the frequencies of a given mode at different temperatures were plotted against the frequencies of the 918 cm^{-1} mode measured on the same spectrum, yielding a plot of the relative shifts which is independent of any temperature estimate; (3) the slope of this relation is the ratio of the temperature shifts of the two modes, and, knowing the absolute shift of the 918 cm^{-1} mode with

good precision, the absolute shift of the other mode can be obtained. The reliability of this method is ensured by the consistency between the frequency shifts obtained directly from the measurements in the high-temperature cell and those obtained indirectly for the intense modes (Fig. 3a). For the weakest modes, the shifts obtained by merging the two sets of data are more reliable because they are determined from more data points (Fig. 3b). These data are summarized in Table 1.

Above 910 K in Experiment 2, a significant transformation to forsterite was observed on the scale of the analyzed area (<5 μm), marked in particular by the appearance of two strong peaks of the olivine structure at about 815 and 845 cm^{-1}. It is difficult to follow the transformation quantitatively because the analyzed volume is small and the amount of transformation varies within the sample. In the first spectrum, in which significant back-transformation was observed, two weak peaks appeared

TABLE 1. Raman mode frequency shifts with temperature in β-Mg$_2$SiO$_4$

ν_i (cm⁻¹)	Expts. 2 and 3			Expt. 1			All expts.	
	$\partial\nu_i/\partial T$ (cm⁻¹·K⁻¹)	η	n	η	n	η	$\partial\nu_i/\partial T$ (cm⁻¹·K⁻¹)	Preferred value (cm⁻¹·K⁻¹)
918	−0.020(2)	—	25	—	12	—	—	−0.020(2)
885	−0.028(5)	1.44	15	—	0	—	—	−0.028(5)
778	−0.029(3)	1.50	22	1.55	12	1.47(12)	−0.029(6)	−0.029(3)
723	−0.018(2)	0.93	25	0.94	12	0.92(8)	−0.018(4)	−0.018(2)
620	−0.015(3)	0.78	18	0.77	10	0.78(12)	−0.015(4)	−0.015(3)
585	−0.007(3)	0.33	16	0.47	9	0.33(11)	−0.007(3)	−0.007(3)
553	−0.022(3)	1.14	22	1.26	12	1.17(9)	−0.023(4)	−0.022(3)
443	−0.028(4)	1.42	22	1.58	11	1.45(13)	−0.028(5)	−0.028(4)
426	−0.017(3)	0.86	14	1.16	10	0.93(16)	−0.018(3)	−0.018(3)
398	−0.033(5)	1.70	10	1.51	12	1.44(19)	−0.028(5)	−0.028(5)
341	−0.30(10)	1.52	9	1.14	6	1.53(50)	−0.030(12)	0.030(10)
262	—	—	0		8	1.04(22)	−0.020(6)	−0.020(6)
231	−0.017(3)	0.88	11	0.97	10	0.89(12)	−0.017(3)	−0.017(3)

Note: n is the number of measurements; η is the ratio of the temperature-induced frequency shift of a given band to the temperature-induced frequency shift of the 918 cm⁻¹ band, all assumed linear.

near 670 and 1010 cm⁻¹, which cannot be attributed to either the β-phase or the olivine. To observe the first step of the transformation, the temperature was held constant at 830 K in Experiment 3 for about 20 min. The resulting spectrum is that of the β-phase, with peaks superimposed at 675 and 1010 cm⁻¹; the strong peaks of forsterite (ambient frequencies of 824 and 856 cm⁻¹) were not observed in this spectrum (Fig. 1a). Upon cooling to ambient temperature, the decrease of the Raman linewidth shows that these peaks are indeed doublets at 665–685 and 1005–1025 cm⁻¹, indicating the formation of an intermediate phase in the transformation process. In Experiment 1, similar features were observed for laser heating temperatures estimated at 800–900 ± 100 K. For temperatures above 1000 ± 100 K, direct transformation to forsterite was observed; no extra peaks were evident. At temperatures near 1200 ± 100 K, the transformation to forsterite was nearly complete within about 1 min.

Ambient-temperature Raman spectra of untransformed and partially back-transformed Ni$_2$SiO$_4$ spinel after 10 min at 1073 K are presented in Figure 4. The spectrum of the untransformed material is consistent with a previous spectrum of Yamanaka and Iishi (1986). The spectrum of the transformed sample corresponds to the olivine form of Ni$_2$SiO$_4$, possibly mixed with residual spinel, with weak but significant bands superimposed at 710, 751, 1000, and 1020 cm⁻¹. These peaks do not belong to either the olivine or spinel structures. Broad peaks are also observed in the 300–600 cm⁻¹ range.

TEM

TEM observations on the β-phase samples heated at 1120 K for 30 min show crystals of untransformed β-phase surrounded by transformed areas from which powder diffraction patterns are obtained (Fig. 5). Some of these patterns were indexed with the forsterite lattice spacing. However, it was also observed that these powder aggre-
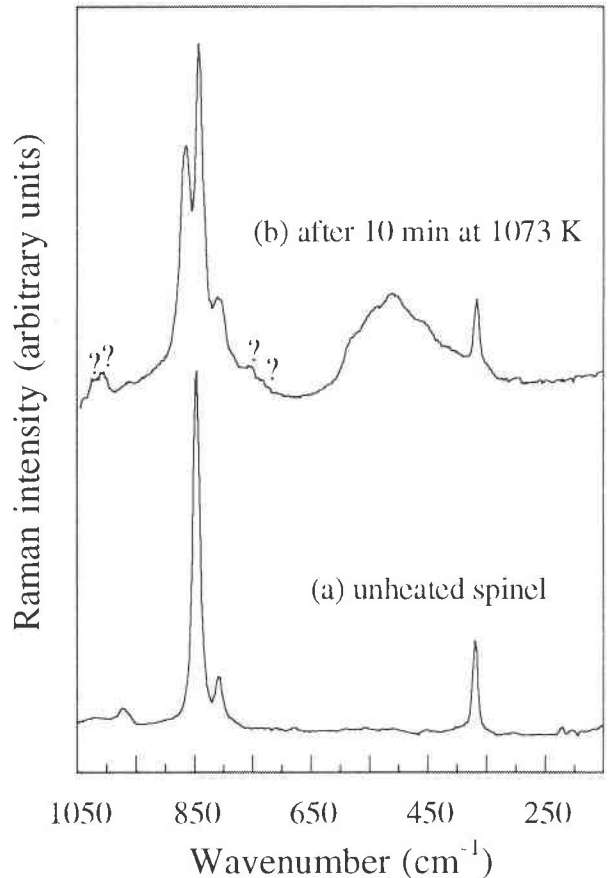

FIGURE 4. Raman spectra of (a) untransformed γ-Ni$_2$SiO$_4$, and (b) the sample after 10 min at 1073 K and 1 atm. Peaks labeled by question marks cannot be attributed to either the olivine or the spinel structure. Notice also the broad feature at about 500 cm⁻¹, which may be attributed to structural disorder in the sample.
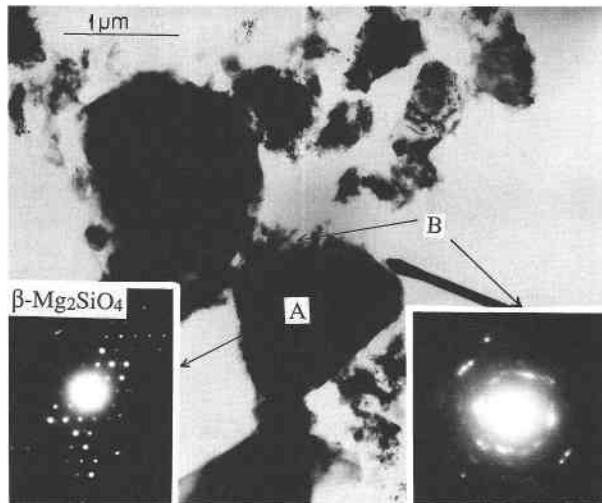
FIGURE 5. TEM micrograph of partially back-transformed β-Mg$_2$SiO$_4$ after 30 min at 1120 K. Diffraction pattern of the center of a micrometer-sized grain (A) corresponds to a single-crystal of untransformed β-Mg$_2$SiO$_4$, whereas diffraction patterns of the rims (B) correspond to powder patterns of transformed material.

gates were very sensitive to electron-beam irradiation and recrystallized within a few seconds. Similar observations were made by McMillan et al. (1991) on a sample heated at 850 K for 5 min. It is thus impossible to detect from TEM the presence of an intermediate phase.

X-ray diffraction

β-Mg$_2$SiO$_4$ persists as a metastable phase up to 973 K within the duration of the experiment. The evolution of unit-cell parameters and volume were followed up to this temperature. The accuracy of these measurements is limited because no internal standard was used to determine precisely the position of the heated sample in the beam. However, our average volumetric thermal expansion, 3.5 $\times$ 10^{-5} K^{-1}, and the relative linear thermal expansions

of the unit-cell parameters agree qualitatively with the results of Suzuki et al. (1980).

Above 973 K β-Mg$_2$SiO$_4$ starts to revert to forsterite within the time of the experiments (typically a few minutes to a few hours). The kinetics were obtained by monitoring the evolution of the forsterite volume fraction with increasing time (Table 2; Fig. 6). The effect of temperature on the back-transformation kinetics is quite dramatic. As already noted, β-Mg$_2$SiO$_4$ does not transform to forsterite up to 973 K within hours, but it takes about 10 h at 1023 K and 5 min at 1118 K to obtain 50% forsterite. A few back-transformation experiments were also performed under vacuum. The effect was to slow down the reaction (Table 2).

KINETICS AND MECHANISMS OF THE BACK-TRANSFORMATION

Structural interpretation of the Raman data

At 910 K in Experiment 2 and at 830 K in Experiment 3 an intermediate phase is formed between the β-phase and forsterite. This phase could be quenched and is characterized by peaks located at 665–685 and 1005–1025 cm^{-1}, which superimpose the characteristic peak of unreacted β-phase and of newly formed forsterite. The positions of these peaks match closely with those of the tetrahedral chain vibrations in orthoenstatite (Chopelas and Boehler 1992). However, the occurrence of orthoenstatite is unlikely for the following reasons: (1) Orthoenstatite is not observed in the starting material, either by X-ray powder and electron diffraction or by Raman spectroscopy; it would have had to form during the back-transformation; (2) Orthoenstatite can form by a metastable disproportionation of the β-phase into MgSiO$_3$ and MgO (which has no Raman spectrum), or it can form if the sample is nonstoichiometric. This is unlikely because of the slow diffusion rates at 830 K. The new peaks are observed not only in samples in which partial transformation to forsterite has occurred but also in samples with no transformation to olivine. Thus, the new peaks are attributed to an intermediate "phase" or to the presence

TABLE 2. Volume fraction of forsterite (X) transformed from β-phase with time (in minutes)

1023 K air		1053 K air		1083 K air		1053 K vacuum		1118 K vacuum	
t	X	t	X	t	X	t	X	t	X
135	0.08	60	0.16	5	0.02	60	0.05	10	0.21
266	0.17	80	0.20	10	0.09	120	0.10	30	0.38
331	0.26	105	0.26	15	0.20	193	0.09	60	0.51
393	0.36	120	0.32	20	0.24	300	0.09		
453	0.40	135	0.36	25	0.41				
515	0.50	160	0.43	30	0.45				
575	0.51	180	0.52	35	0.59				
640	0.52	200	0.60	40	0.63				
770	0.67	220	0.68	45	0.62				
1045	0.76	240	0.70						
		270	0.75						
		300	0.77						

of defects in the β-phase prior to the conversion to forsterite.

The frequencies of the new peaks are similar to those of orthoenstatite, suggesting that the defect structure or phase involves a high degree of polymerization of SiO_4 tetrahedra. This intermediate phase could be a structurally disordered β-phase with a high density of planar defects that have the ω or ϵ^* structure, postulated by Hyde et al. (1982) and Madon and Poirier (1983) as an intermediate phase in the α-β martensitic transformation. Because this phase or defect structure is closely related to the β-phase structure, it would be nearly indistinguishable on X-ray diffraction patterns. However, it can explain the irreversible change in lattice parameters near 825 K in the β-phase observed by Tsukimura et al. (1988). The occurrence of a similar phase has been proposed in the high-pressure transformations of Mg_2GeO_4 olivine (Reynard et al. 1994) and may explain the high-pressure transformation observed in forsterite by Raman spectroscopy (Durben et al. 1993). However, the peaks that appear at high pressure in forsterite occur at about 750 and 950 cm^{-1} and not at 670 and 1020 cm^{-1}. This discrepancy may indicate that the structural modifications observed at high pressure and ambient temperature in forsterite and at high temperature and ambient pressure in the β-phase are different. These frequency differences may also be due to the difference in local environment around defects in forsterite and β-phase and the different conditions of the experiments, e.g., different Si-O-Si bond angles in the tetrahedral chains could account for the discrepancy.

The peaks at 665–685 and 1005–1025 cm^{-1} are observed only when the transformation occurs between about 800 and 1000 K. Indeed, the higher the temperature, the weaker these peaks are and the greater the back-transformation that occurs to forsterite. In Experiment 1, direct transformation to forsterite is observed within seconds at estimated temperatures between 1000 and 1200 K. It suggests that the transformation mechanism changes with increasing temperature from one involving an intermediate defect phase at intermediate temperatures to a direct nucleation and growth of forsterite at temperatures above about 1000 K. These observations are consistent with the in-situ high-temperature single-crystal X-ray diffraction study of Tsukimura et al. (1988). At 825 K, they observed a deterioration of the crystal quality, marked by a broadening and weakening of the diffraction peaks and by a discontinuous change of the unit-cell parameters. At 1100 K, they observed a replacement of the diffraction peaks from the β-phase by powder rings of forsterite. Further structural characterization (e.g., Rietveld analysis or single-crystal studies) is desirable to determine the nature of the intermediate phases.

The weak features observed in the frequency ranges 700–800 and 1000–1050 cm^{-1} in the spectrum of partially transformed Ni_2SiO_4 spinel also cannot be attributed to the olivine or spinel structure. Once again, the observed frequencies indicate the presence of defects
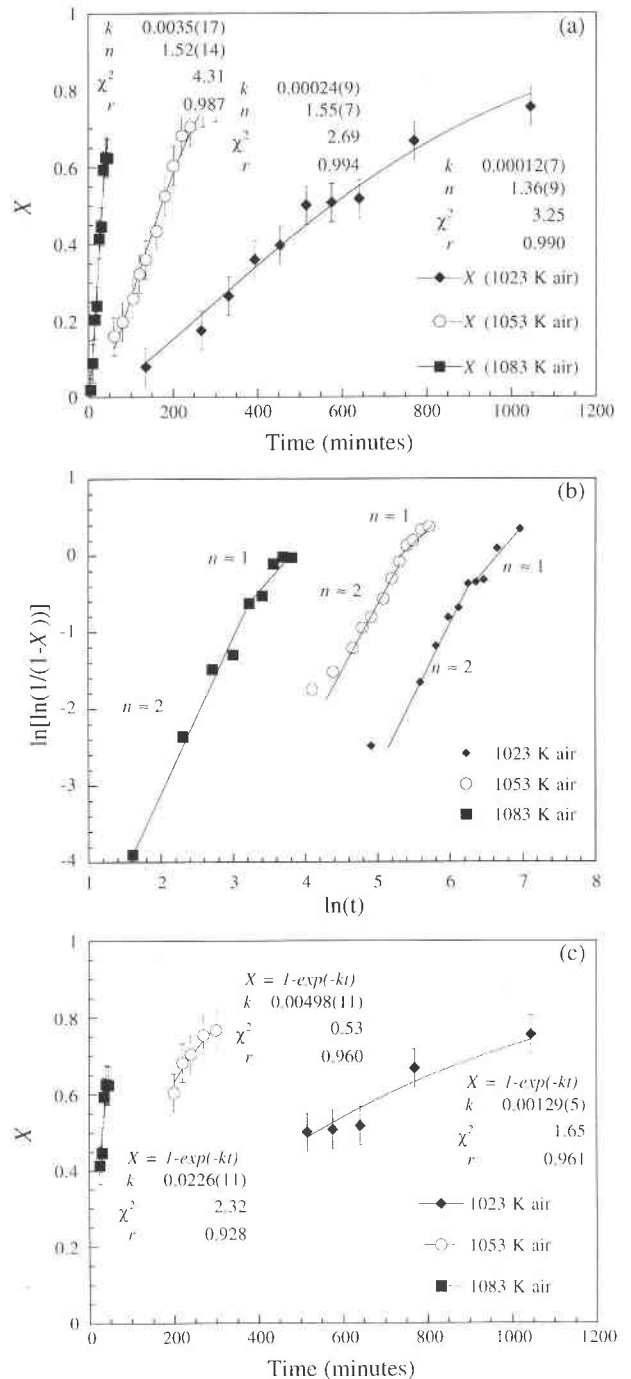

FIGURE 6. Kinetics of the back-transformation of β-Mg_2SiO_4 to forsterite. (**a**) All data obtained in air with fits to the general Avrami equation (see text); X is the volume fraction of transformed material. (**b**) Logarithmic plot showing the change from a regime with $n > 1$ at low transformed fractions to a regime with $n \approx 1$ at high transformed fractions. (**c**) Fits to the data corresponding to the second regime in **b**; n fixed at one.
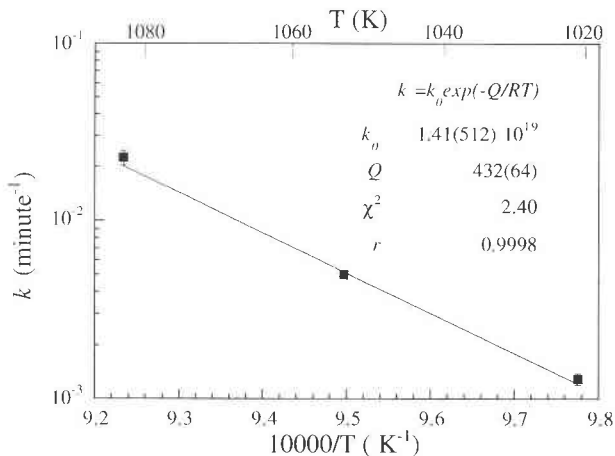
FIGURE 7. Plot of the reaction constant K against inverse temperature determined from the kinetic data in air assuming n = 1. An activation energy of 432 ± 64 kJ/mol is obtained for the growth process.

characterized by Si-O-Si linkages, such as those formed during a martensitic transformation mechanism. In addition, the presence of broad bands at low frequencies is consistent with the observation of decreasing diffraction intensity and increasing site disorder in heated Ni$_2$SiO$_4$ spinel, which can be explained by the presence of numerous randomly distributed stacking faults involved in the spinel to olivine back-transformation (Yamanaka 1986). Thus, such defects formed during the back-transformation to olivine always have the spinel or β-phase structure and are independent of the chemical system and the starting material. If the formation of the defects is actually caused by a martensitic mechanism, this can be operative in any transformation involving an olivine structure and a stable high-pressure spinelloid structure.

Analysis of kinetic data

The kinetic data obtained by X-ray diffraction on the back-transformation of β-Mg$_2$SiO$_4$ to forsterite were analyzed using the classical Avrami equation (see Rubie and Thompson 1985), in which the fraction of transformed material, X, after time t is expressed as

$$X = 1 - \exp(-kt^n) \qquad (1)$$

where k is a reaction constant and n is a critical exponent, both dependent on the reaction mechanism and intensive parameters such as temperature and differential stress. Average values of k and n were obtained from least-squares analysis of the kinetic data at three temperatures (Fig. 6a). The average n is approximately 1.5 for all temperatures. However, plots of $\ln[\ln(1/1 - X)]$ vs. $\ln t$ show breaks in slope suggesting that the kinetic data at each temperature can be separated into two regimes (Fig. 6b). The first regime at the beginning of the transformation ($X < 0.5$) is characterized by $n > 1$, and the second regime at high transformed fractions is characterized by $n \approx 1$. A decrease of n with increasing transformed fraction was

also observed by Rubie et al. (1990) in their study of the olivine-spinel transition in Ni$_2$SiO$_4$, which was conducted with relatively large overstepping of the equilibrium conditions.

The first regime may correspond to the stage in which the reaction kinetics are dominated by nucleation processes [n = 4 for grain-boundary nucleation (Cahn 1956), and n = 2 for nucleation and growth on planar defects (Avrami 1939, 1940, 1941), which are suggested by the Raman data]. The second regime may correspond to the stage in which nucleation-site saturation occurs, and the kinetics are dominated by growth processes, with a typical exponent of one (Cahn 1956). In practice, the exponent n cannot be used to infer the reaction mechanism. For example, an exponent of one is also characteristic of a martensitic mechanism (Poirier 1981b).

Following Rubie et al. (1990), the general rate equation derived by Cahn (1956) could be used to optimize the determination of the nucleation and growth rate from the present kinetic data. We did not use this procedure because we have no evidence that the grain-boundary nucleation and growth mechanism used in the rate equation of Cahn (1956) is appropriate for the present case. However, if we assume n = 1 for the data corresponding to the second regime described above, the temperature dependence of the reaction constant K can be determined (Fig. 6c). The temperature dependence of the reaction constant is a function of (1) a term describing the thermal activation of the transformation process and (2) a term that is related to the overstepping of the equilibrium conditions. The second term takes a different form in the case of an interface-controlled polymorphic phase transition (Carlson and Rosenfeld 1981) vs. martensitic transformation (Poirier 1981b; Madon and Gillet 1984). However, it is nearly constant in the pressure-temperature range investigated here. The reaction constant expression therefore reduces to a form that is characteristic of a thermally activated process, i.e., the growth process. Only the expression of the preexponential constant differs from one mechanism to the other. From an Arrhenius plot (Fig. 7), an activation energy of 432 ± 64 kJ/mol is obtained. This estimate, which is independent of an assumed reaction mechanism, is remarkably close to the activation energy of 438 ± 199 kJ/mol determined for growth in the olivine to spinel transformation in Ni$_2$SiO$_4$ (Rubie et al. 1990). The similarity may be fortuitous owing to the large uncertainties, as well as the differences in the material, the sense of the reaction, and the experimental conditions (e.g., grain size, air vs. buffered f_{O_2}, powder vs. sintered material, etc.). This large activation energy is consistent with the Raman observations that the β-phase transforms to olivine within one minute at temperatures of ~1200 K.

The data obtained in vacuum are too limited to allow a determination of both the activation energy and the preexponential factor. However, there is a significant difference in the kinetics of the back-transformation in air and in vacuum. To give an estimate of this difference, we assumed that the activation energy is similar in air and

TABLE 3. Anharmonic and mode Gruneisen parameters for β-Mg$_2$SiO$_4$

ν_i (cm^{-1})	γ_{iP}	γ_{iT}*	a_i (10^{-5} K^{-1})
918	1.0(2)	0.83(1)	−0.4(7)
885	1.5(3)	0.8	−1.2(12)
778	1.8(2)	1.07(1)	−1.6(8)
723	1.2(2)	0.80(1)	−0.9(7)
620	1.2(3)	0.69(2)	−1.1(11)
585	0.5(2)	0.53(1)	0.0(7)
553	2.0(4)	1.34(1)	−1.3(11)
443	3.0(6)	1.35(2)	−3.5(20)
426	1.9(4)	0.97(2)	−1.9(15)
398	3.4(9)	1.37(2)	−4.2(32)
341	4.3(13)	1.36(3)	−5.9(44)
262	3.8(11)	1.19(14)	−5.3(42)
231	3.7(9)	1.25(2)	−4.9(30)

* From Chopelas (1991).

vacuum. This leads to a preexponential factor that is one order of magnitude smaller at 10^{-2} Pa than in air. This suggests a significant effect of either the O$_2$ or the H$_2$O partial pressure on the kinetics of the back-transformation. Further experimental studies are needed to address this problem.

HIGH-TEMPERATURE THERMODYNAMIC PROPERTIES OF β-Mg$_2$SiO$_4$

From the frequency shifts with temperature, the isobaric mode parameters (Mammone and Sharma 1979; Gillet et al. 1989) are given by

$$\gamma_{iP} = (\partial \ln \nu_i / \partial \ln V)_P = (1/\alpha)(\partial \ln \nu_i / \partial T)_P \qquad (2)$$

where ν_i is the frequency of the ith mode and α the thermal expansivity. Using the isothermal mode Grüneisen parameters (γ_{iT}) from Chopelas (1991), the intrinsic anharmonic mode parameters are given by (Mammone and Sharma 1979; Gillet et al. 1989)

$$a_i = (\partial \ln \nu_i / \partial T)_V = \alpha(\gamma_{iT} - \gamma_{iP}). \qquad (3)$$

Their absolute values (Table 3) are, on average, higher by about 1×10^{-5} K^{-1} than those for forsterite, but this difference is within the experimental uncertainties. These parameters are significantly different from zero for many modes in both phases, indicating significant intrinsic anharmonic behavior. This behavior can be accounted for in the expression for the constant-volume heat capacities (C_V) at high temperatures to correct for intrinsic anharmonic effects (e.g., Gillet et al. 1991; Fiquet et al. 1992)

$$C_{Va} = \Sigma_i \, C_{Vhi}(1 - 2a_i T) \qquad (4)$$

where the h and a subscripts refer to the harmonic and corrected anharmonic heat capacities, respectively. In the high-temperature limit ($C_{Vhi} \approx kT$), at which anharmonic effects become significant, Equation 4 becomes

$$C_{Va} = C_{Vh}(1 - 2\bar{a}T) \qquad (5)$$

where $\bar{a}$ is the arithmetic mean of the anharmonic parameters. Because the mean anharmonic parameter for the
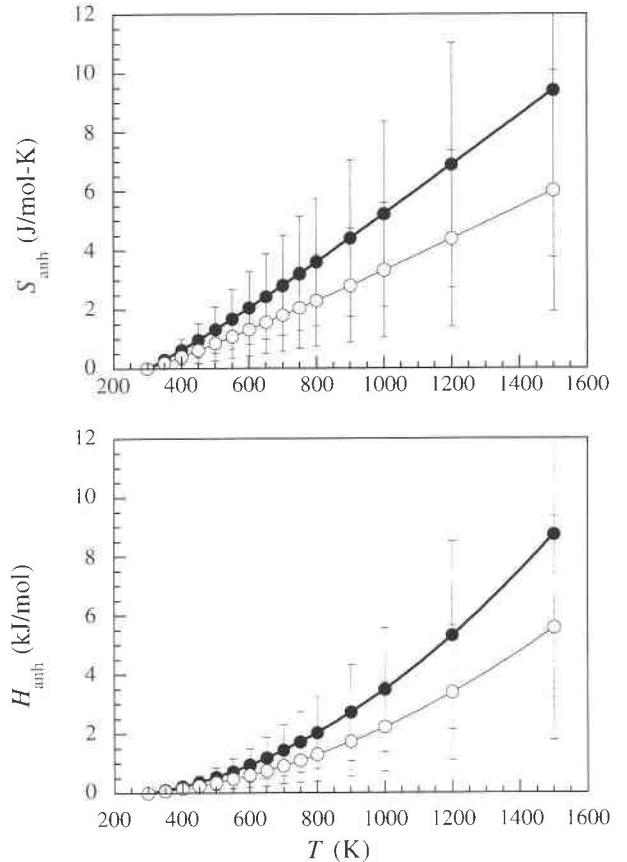
FIGURE 8. Intrinsic anharmonic contributions to the entropies and enthalpies of β-Mg$_2$SiO$_4$ (solid circles) and forsterite (open circles). The corrections are greater for β-Mg$_2$SiO$_4$, but the error bars for the two phases overlap.

β-phase is 1.0×10^{-5} K^{-1} lower than for forsterite, the anharmonic corrections to C_V are higher for the β-phase. However, when the uncertainties of the anharmonic parameters are taken into account, the effects of intrinsic anharmonicity on the standard entropies [$\sim -6n\bar{R}a(T - 298.15)$] and relative enthalpies [$\sim -3n\bar{R}a(T^2 - 298.15^2)$] are not significantly different for the β-phase and for forsterite (Fig. 8). Thus, it is difficult to quantify precisely the effect of intrinsic anharmonicity on the position and slope of the equilibrium curve between α- and β-Mg$_2$SiO$_4$.

REFERENCES CITED

Akaogi, M., Ito, E., and Navrotsky, A. (1989) Olivine-modified spinel-spinel transitions in the system Mg$_2$SiO$_4$-Fe$_2$SiO$_4$: Calorimetric measurements, thermochemical calculation, and geophysical application. Journal of Geophysical Research, 94, 15671–15685.

Avrami, M. (1939) Kinetics of phase change: I. General theory. Journal of Chemical Physics, 7, 1103–1112.

——— (1940) Kinetics of phase change: II. Transformation-time theory for random distribution of nuclei. Journal of Chemical Physics, 8, 212–224.

——— (1941) Kinetics of phase change: III. Granulations, phase change, and microstructure. Journal of Chemical Physics, 9, 177–184.

Boland, J.N., and Liebermann, R.C. (1983) Mechanism of the olivine to spinel transformation in Ni$_2$SiO$_4$. Geophysical Research Letters, 10, 87–90.

Boland, J.N., and Liu, L. (1983) Olivine to spinel transformation in Mg$_2$SiO$_4$ via faulted structures. Nature, 303, 233–235.

Brearley, A.J., Rubie, D.C., and Ito, E. (1992) Mechanisms of the transformations between the α, β and γ polymorphs of Mg$_2$SiO$_4$ at 15 GPa. Physics and Chemistry of Minerals, 18, 343–358.

Burnley, P.C., and Green, H.W. (1989) Stress dependence of the olivine-spinel transformation. Nature, 338, 753–756.

Cahn, J.W. (1956) The kinetics of grain boundary nucleated reactions. Acta Metallica, 4, 449–459.

Carlson, W.D., and Rosenfeld, J.L. (1981) Optical determination of topotactic aragonite-calcite growth kinetics: Metamorphic implications. Journal of Geology, 89, 615.

Chopelas, A. (1991) Thermal properties of β-Mg$_2$SiO$_4$ (modified spinel) at mantle pressures derived from vibrational spectroscopy: Implications for the mantle at 400 km. Journal of Geophysical Research, 96, 11817–11830.

Chopelas, A., and Boehler, R. (1992) Raman spectroscopy of MgSiO$_3$ phases synthesized in a CO$_2$ laser heated diamond anvil cell: Perovskite and clinopyroxene. In Geophys Monograph, 67, 101–108.

Durben, D.J., McMillan, P.F., and Wolf, G.H. (1993) Raman study of the high-pressure behavior of forsterite (Mg$_2$SiO$_4$) crystal and glass. American Mineralogist, 78, 1143–1148.

Fiquet, G., Gillet, P., and Richet, P. (1992) Anharmonic contributions to the heat capacity of minerals at high-temperatures: Application to Mg$_2$GeO$_4$, Ca$_2$GeO$_4$, MgCaGeO$_4$. Physics and Chemistry of Minerals, 18, 469–479.

Gillet, P., Guyot, F., and Malezieux, J.M. (1989) High-pressure and high-temperature Raman spectroscopy of Ca$_2$GeO$_4$: Some insights on anharmonicity. Physics of the Earth and Planetary Interiors, 58, 141–154.

Gillet, P., Richet, P., Guyot, F., and Fiquet, G. (1991) High-temperature thermodynamic properties of forsterite. Journal of Geophysical Research, 96, 11805–11816.

Guyot, F., Gwanmesia, G.D., and Liebermann, R.C. (1991) An olivine to beta phase transformation mechanism in Mg$_2$SiO$_4$. Geophysical Research Letters, 18, 89–92.

Gwanmesia, G.D., Liebermann, R.C., and Guyot, F. (1990) Hot-pressing and characterization of polycrystals of b-Mg$_2$SiO$_4$ for acoustic velocity measurements. Geophysical Research Letters, 17, 1331–1334.

Hyde, B.G., White, T.J., O'Keeffe, M., and Johnson, A.W.S. (1982) Structures related to those of spinel and the β-phase, and a possible mechanism for the transformation olivine-spinel. Zeitschrift für Kristallographie, 160, 53–62.

Katsura, T., and Ito, E. (1989) The system Mg$_2$SiO$_4$-Fe$_2$SiO$_4$ at high pressures and temperatures: Precise determinations of stabilities of olivine, modified spinel and spinel. Journal of Geophysical Research, 94, 15663–15670.

Lacam, A., Madon, M., and Poirier, J.P. (1980) Olivine glass and spinel formed in laser heated, diamond anvil high-pressure cell. Nature, 228, 155–157.

Madon, M., and Poirier, J.P. (1983) Transmission electron microscopy observation of α, β and γ (Mg,Fe)$_2$SiO$_4$ in shocked meteorites: Planar defects and polymorphic transitions. Physics of the Earth and Planetary Interiors, 33, 31–44.

Madon, M., and Gillet, P. (1984) A theoretical approach to the kinetics of calcite ↔ aragonite transition: Application to laboratory experiments. Earth and Planetary Science Letters, 67, 400–414.

Madon, M., Guyot, F., Peyronneau, J., and Poirier, J.P. (1989) Electron microscopy of high-pressure phases synthesized from natural olivine in diamond anvil cell. Physics and Chemistry of Minerals, 16, 320–330.

Mammone, J.F., and Sharma, S.K. (1979) Pressure and temperature dependence of the Raman spectra of rutile-structure oxides. Carnegie Institution of Washington Year Book, 78, 369–373.

McMillan, P.F., and Akaogi, M. (1987) Raman spectra of β-Mg$_2$SiO$_4$ (modified spinel) and γ-Mg$_2$SiO$_4$ (spinel). American Mineralogist, 72, 361–364.

McMillan, P.F., Akaogi, M., Sato, R.K., Poe, B., and Foley, J. (1991) Hydroxyl groups in β-Mg$_2$SiO$_4$. American Mineralogist, 76, 354–360.

Poirier, J.P. (1981a) Martensitic olivine spinel transformation and plasticity of the mantle transition zone. In Anelasticity in the Earth, 4, 113–117.

——— (1981b) On the kinetics of olivine-spinel transition. Physics of the Earth and Planetary Interiors, 26, 179–185.

Price, G.D. (1983) The nature and significance of stacking faults in wadsleyite, natural β-(Mg,Fe)$_2$SiO$_4$ from the Peace River meteorite. Physics of the Earth and Planetary Interiors, 33, 137–147.

Price, G.D., Putnis, A., Agrell, S.O., and Smith, D.G.W. (1983) Wadsleyite, natural β-(Mg,Fe)$_2$SiO$_4$ from the Peace River meteorite. Canadian Mineralogist, 21, 29–35.

Remsberg, A.R., Boland, J.N., Gasparik, T., and Liebermann, R.C. (1988) Mechanism of the olivine-spinel transformation in Co$_2$SiO$_4$. Physics and Chemistry of Minerals, 15, 498–506.

Reynard, B. (1993) Infrared reflectivity of γ-(spinel)Ni$_2$SiO$_4$. European Journal of Mineralogy, 5, 31–35.

Reynard, B., Petit, P.E., Guyot, F., and Gillet, P. (1994) Pressure-induced structural modifications in Mg$_2$GeO$_4$-olivine: A Raman spectroscopic study. Physics and Chemistry of Minerals, 20, 556–562.

Rubie, D.C., and Thompson, A.B. (1985) Kinetics of metamorphic reactions at elevated temperatures and pressures: An appraisal of experimental data. In Advances in Physical Geochemistry, 4, 291 p.

Rubie, D.C., and Champness, P.E. (1987) The evolution of microstructure during the transformation of Mg$_2$GeO$_4$ olivine to spinel. Bulletin de Minéralogie, 110, 471–480.

Rubie, D.C., Tsuchida, Y., Yagi, T., Utsumi, W., Kikegawa, T., Shimomura, O., and Brearley, A.J. (1990) An in situ X ray diffraction study of the kinetics of the Ni$_2$SiO$_4$ olivine-spinel transformation. Journal of Geophysical Research, 95, 15829–15844.

Suzuki, I., Ohtani, E., and Kumazawa, M. (1980) Thermal expansion of modified spinel, β-Mg$_2$SiO$_4$. Journal of Physics of the Earth, 28, 273–280.

Tsukimura, K., Sato-Sorensen, Y., Ghose, S., and Sawamoto, H. (1988) High-temperature single-crystal study of β-Mg$_2$SiO$_4$. Eos, 69, 498.

Vaughan, P.J., Green, H.W., and Coe, R.S. (1982) Is the olivine-spinel phase transformation martensitic? Nature, 298, 357–358.

——— (1984) Anisotropic growth in the olivine-spinel transformation of Mg$_2$GeO$_4$ under nonhydrostatic stress. Tectonophysics, 108, 299–322.

Watanabe, H. (1982) Thermochemical properties of synthetic high-pressure compounds relevant to the Earth's mantle. In S. Akimoto and M.H. Manghnani, Eds., High-pressure research in geophysics, p. 441–464. Center for Academic Publications, Tokyo.

Will, G., and Lauterjung, J. (1987) The kinetics of the pressure-induced olivine-spinel phase transition in Mg$_2$GeO$_4$. In M.H. Manghnani and Y. Syono, Eds., High pressure in mineral physics, p. 177–186. AGU, Washington, DC.

Yamanaka, T. (1986) Crystal structures of Ni$_2$SiO$_4$ and Fe$_2$SiO$_4$ as a function of temperature and heating duration. Physics and Chemistry of Minerals, 13, 227–232.

Yamanaka, T., and Iishi, M. (1986) Raman scattering and lattice vibrations of Ni$_2$SiO$_4$ spinel at elevated temperature. Physics and Chemistry of Minerals, 13, 156–160.